Genome-wide identification and expression analysis of the *CLC* gene family in pomegranate (*Punica granatum*) reveals its role in salt resistance

Cuiyu Liu
Nanjing Forestry University
Yujie Zhao
Nanjing Forestry University
Xueqing Zhao
Nanjing Forestry University
Jianmei Dong
Nanjing Forestry University
Zhaohe Yuan (zhyuan88@hotmail.com)
Nanjing Forestry University

Research article

Keywords: CLC gene family, phylogenetic analysis, anion content, expression pattern, NaCl stress

Posted Date: August 27th, 2020

DOI: https://doi.org/10.21203/rs.3.rs-54027/v1

Version of Record: A version of this preprint was published at BMC Plant Biology on December 11th, 2020. See the published version at https://doi.org/10.1186/s12870-020-02771-z.

Abstract

Backgrounds

Pomegranate (*Punica granatum* L.) is an important commercial fruit tree, with moderate tolerance to salinity. The balance of Cl^- and other anions in pomegranate tissues are affected by salinity, however, the accumulation patterns of anions are poorly understood. The chloride channel (CLC) gene family is involved in conducting Cl^-, NO_3^-, HCO_3^- and I^-, but its characteristics have not been reported on pomegranate.

Results

In this study, we identified seven *PgCLC* genes, consisting of four antiporters and three channels, based on the presence of the gating glutamate (E) and the proton glutamate (E). Phylogenetic analysis revealed that seven PgCLCs were divided into two clades, with clade I containing the typical conserved regions GxGIPE (I), GKxGPxxH (II) and PxxGxLF (III), whereas clade II not. Multiple sequence alignment revealed that PgCLC-B had a P [proline, Pro] residue in region I, which is suspected to be a NO_3^-/H^+ exchanger, while PgCLC-C1, PgCLC-C2, PgCLC-D and PgCLC-G contained a S [serine, Ser] residue, with a high affinity to Cl^-. We were determined the content of Cl^-, NO_3^-, $H_2PO_4^-$, and SO_4^{2-} in pomegranate tissues after 18 days of salt treatments (0, 100, 200 and 300 mM NaCl). Compared with control, the Cl^- content increased sharply in tissues and was ranked as leaf > stem > root. The uptake of NO_3^- and SO_4^{2-} was inhibited by high salinity, while that of $H_2PO_4^-$ increased. The results of real-time reverse transcription PCR (qRT-PCR) revealed that *PgCLC* genes had tissue-specific expression patterns. The high expression levels of *PgCLC-C1*, *PgCLC-C2* and *PgCLC-D* in leaves suggested they played roles in sequestrating Cl^- into the vacuoles. However, the low expression levels of *PgCLCs* in roots might be contributed to the exclusion of Cl^- from root cells. Also, the non-significantly changed concentration of NO_3^- in leaves and the up-regulated *PgCLC-B* indicated an acceleration of transporting NO_3^- into leaves to mitigate the nitrogen deficiency.

Conclusions

Our findings suggested that *PgCLC* genes played important roles in balance of Cl^- and NO_3^- in pomegranate tissues under salt stress. This study establishes a theoretical foundation for the further functional characterization of *CLC* genes in pomegranate.

Background

Chlorine is an essential micronutrient for plants, predominantly occurring in the form of the chloride anion (Cl^-) [1, 2]. Cl^- is mainly involved in plant physiological activities, such as photosynthesis, regulation of stomatal opening and closing, stabilization of the membrane potential, regulation of intracellular pH gradients and electrical excitability [2]. Excess and/or deficiency of Cl^- leads to weak plant growth, low yield and poor quality [3, 4]. Under a hypersaline condition (a high concentration of NaCl), plants maintain a balance of Na^+ and Cl^- at the cellular and the whole plant levels by excluding Na^+ and Cl^- from the cell or

sequestering them into the vacuoles and controlling Na^+ and Cl^- transport from roots to the acrial parts [3, 5]. Previous studies on plant salt tolerance mostly focused on the effects of Na^+, while few studies on Cl^- toxic effects [6].

Pomegranate (*Punica granatum* L.) is a salt-tolerant plant that is widely grown in arid and semiarid regions [7]. In our previous study, we found that the Cl^- content was two times more than Na^+ content in pomegranate tissues, and the accumulation of other anions was also affected by various concentration of salinity [8]. CLC proteins are highly associated with uptake and transport of these anions, like Cl^-, NO_3^-, HCO_3^-, I^-, and Br^- [9–12]. However, the characteristics of *CLC* genes have not been reported on pomegranate. This study aimed to make a comprehensive, genome-wide inventory of the CLC gene family in pomegranate and to illuminate their roles in responses to NaCl stress.

The first chlorine channel (CLC) family gene (*CLC-0*) was identified from the electric organ of the marine ray (*Torpedo marmorata*) [13], and since then, some new members have been found in bacteria, yeast, mammals and plants [14]. In land plants, the first CLC gene, *CLC-Nt1*, was cloned in tobacco [15]. Subsequently, numerous CLC gene homologues were isolated from *Arabidopsis* [16], rice (*Oryza sativa*) [17], soybean and trifoliate orange (*Poncirus trifoliata*) [18], etc. All of the CLC proteins have a highly conserved voltage-gated chloride channel (Voltage-gate CLC) domain and two CBS (cystathionine beta synthase) domains of putative regulatory function [9]. CLC proteins may act as Cl^- channels or as Cl^-/H^+-exchangers (antiporters) [14]. The CLC gene family contains three highly conserved regions related to anion selectivity: GxGIPE (I), GKxGPxxH (II) and PxxGxLF (III) [19]. If the x residue in the conserved region (I) is P [proline, Pro], NO_3^- is preferentially transported, whereas if it is substituted by S [serine, Ser], Cl^- is preferentially transported[20]. The first x residue in conserved region II and the next fourth residue of the conserved region III can both be E (Glu) residue, which are signatures for CLC antiporters [21, 22]. However, if any other amino acids are found at these positions, such as in AtCLCe, AtCLCf and AtCLCg, the CLC proteins may exert CLC channels activity [22]. The Cl^- channels mediate passive transport by dissipating pre-existing electrochemical gradients, while the antiporters mediate active transport by coupling with energy consumption to move the substrate against an electrochemical gradient [22]. In higher plants, CLC proteins are localized to the organelles membranes, including the plasma membrane, vacuole membrane, endoplasmic reticulum membrane, mitochondrial membrane, chloroplast membrane, etc[14]. These proteins play vital roles in the control of electrical excitability, turgor maintenance, stomatal movement, and ion homeostasis, as well as in responses to biotic and/or abiotic stress [23–25].

In *Arabidopsis*, there are seven reported CLCs: AtCLCa ~ AtCLCg, which play different roles in diverse cell organelles [26, 27]. Barbierbrygoo *et al*. [28] and Marmagne *et al*.[29] suggested that AtCLCa ~ AtCLCd and AtCLCg were clustered into a distinct branch, belonging to eukaryotic CLCs, while AtCLCe and AtCLCf are closely related to prokaryotic CLC channels. AtCLCa is an NO_3^-/H^+ exchangers localized in the vacuolar membrane, which is critically involved in this nitrate accumulation in the vacuole [16]. AtCLCb, a vacuolar antiporter that shares 80% identity with AtCLCa, is highly expressed in young roots, hypocotyl and cotyledons [27]. AtCLCc is essential for the detoxification of the cytosol by sequestrating Cl^- into the vacuoles under salt stress, and it is strongly expressed in guard cells, pollen and roots [23]. AtCLCd and

AtCLCf, both localized in Golgi membranes, may play a role in the acidification of the *trans*-Golgi vesicles network [29, 30], while AtCLCe is targeted to the thylakoid membranes in chloroplasts [29]. AtCLCg, the closest homolog to AtCLCc (62% identity), plays a physiological role in the Cl^- homeostasis during NaCl stress [31]. In other plants, many *CLC* genes are involved in anions transport and in the response to salt stress. For instance, the expression level of *OsCLC-1* is upregulated in rice under NaCl stress [17]; *PtrCLC* genes are profoundly induced in orange by salt stress[18]; *GmCLC1* has been found to enhanced salt tolerance in transgenic *Arabidopsis* seedlings by reducing the Cl^- accumulation in shoots[6]; and *GsCLC-c2* over-expression contributes to Cl^- and NO_3^- homeostasis, and therefore confers wild soybean the salt tolerance[32].

Results

Identification of CLCs in pomegranate

A HMM profile was used to identify the putative *CLC* genes in the pomegranate genome. All seven putative *CLC* genes contained a highly conserved Volgate_CLC domain and two CBS domains, and they were named *PgCLC-B* to *PgCLC-G* according to the homologous *AtCLCs* (Table 1). The analysis of protein sequences showed that the PgCLCs contained 698 ~ 797 amino acids and had molecular weights of 75.7 ~ 87.9 kDa. The predicted isoelectric points (pI) of all the PgCLC proteins ranged from 5.86 to 8.44. The grand average of the hydrophobicity (GRAVY) values were all positive values, indicating that the PgCLCs were hydrophobic proteins. There were a number of transmembrane helices (TMs) in the PgCLCs, ranging from 9 to 11, which were associated with their location in the organelles membrane: six of PgCLCs were located on the plasma membrane and PgCLC-E was located on the chloroplast thylakoid membrane.

Table 1. Characteristics of the *CLC* genes in pomegranate

Gene ID	Name	AA	Mw(kDa)	pI	GRAVY	Orthologs	TMs	Subcellular location
CDL15_Pgr005627	*PgCLC-B*	797	87.9	6.49	0.259	*AtCLC-B*	9	Plasma membrane
CDL15_Pgr027626	*PgCLC-C1*	698	75.7	7.53	0.364	*AtCLC-C*	10	Plasma membrane
CDL15_Pgr013895	*PgCLC-C2*	717	78.1	5.92	0.325	*AtCLC-C*	10	Plasma membrane
CDL15_Pgr008552	*PgCLC-D*	788	86.9	8.57	0.175	*AtCLC-D*	11	Plasma membrane
CDL15_Pgr019810	*PgCLC-E*	764	81.3	5.86	0.188	*AtCLC-E*	10	Chloroplast thylakoid membrane
CDL15_Pgr012201	*PgCLC-F*	765	81.7	6.54	0.035	*AtCLC-F*	11	Plasma membrane
CDL15_Pgr015371	*PgCLC-G*	709	77.3	8.44	0.468	*AtCLC-G*	10	Plasma membrane

Phylogenetic analysis of the CLC gene family in pomegranate

To elucidate the evolutionary traits of the CLC gene family in land plants, we investigated fifteen interesting species that had available reference genome sequences. Our results showed two obvious clades of the CLC gene tree, clade I was the major group bearing a moderate support (BS=61%, Fig. S1) and clade II contained two subgroups (Fig. 1). The divergence of clades I and II might have occurred before the origin of land plants due to each clade consisting of taxa from embrophytes (Fig. 1). Phylogenetic analyses indicated multiple rounds of ancient gene expansion (Fig. 1). The diversity of gene copy number from different lineages (Fig.1A). The gene tree-species tree reconcilably identified a gene duplication (the red star in Fig.1B) with a strongly supported (BS=100, Fig.S1) topology of (core eudicots, core eudicots). A gene duplication (the purple star in Fig.1B) resulting in a topology of ((core eudicots, monocots), (core eudicots, monocots)) was identified as one duplicate shared by angiosperms. Our phylogenetic analyses also found gene expansion in seed plants, with a gene birth from an ancient gene duplication (the green star in Fig.1B) and a subsequent gene death. The tree topology [(angiosperms, gymnosperms) angiosperms] of the CLC-A/B/C/G genes (Fig.1) exhibited a gene loss event in gymnosperms.

Here, our phylogenetic results showed that seven putative *CLC* genes in the pomegranate genome originated before the divergence of land plants and were retained after experiencing six times of duplications, including at least one ancient core eudicots-specific duplication and one angiosperm-specific expansion (Fig. 1, Fig. S1).

Conserved motifs and residues of the CLC gene family

To further investigate the structural diversity of all CLCs in land plants, the conserved motifs and regions were analyzed. Here, a total of 10 motifs were selected, referring as motif 1-10, and five representative species of each taxa were shown (Fig. 2B, Fig. S1B). Different motif patterns were clearly observed in the two clades, as mentioned above (Fig. 1B). For clade I, most of the CLCs possessed 10 motifs (Fig. 2B, C; Fig. S2). For clade II, most of the CLC-E and CLC-F proteins possessed four motifs: 6, 1, 8 and 2, which were shared by all of the CLCs of clade I. Three conserved regions GxGIPE (I), GKxGPxxH (II) and PxxGxLF (III) were included in motif 9, motif 6 and motif 1, respectively (Fig. 2B, C and D). Three highly conserved regions of the CLC gene family were shared by members of clade I, whereas they were not shared by members of clade II (Fig. 2B, C; Fig. S2).

Additionally, to meticulously analyze the conserved regions of CLC proteins, multiple sequence alignment was performed. Members of the CLC-A/B subfamily had a P [proline, Pro] residue in the conserved region GxGIPE (I), while other proteins of the CLC-C, CLC-G and CLC-D subfamilies in clade I had a S [serine, Ser] residue in the conserved region I (Fig. 3A). These critical residues were recognized to have a close relation with anion selectivity. The P [proline, Pro] preferentially transported NO_3^-, whereas the S [serine, Ser] preferentially transported Cl^- (Fig. 3A). The presence of the conserved gating glutamate (E) in conserved region (II) and the proton glutamate (E) residues in the next fourth residue of the conserved region (III) were signatures for CLC antiporters. Otherwise, the conserved gating glutamate (E) of CLC-G subfamily and the proton glutamate (E) residue of CLC-E and CLC-F subfamilies were substituted by other amino acids (Fig. 3A), which suggested that the members of these three subfamilies might be CLC ion channels. Based on these results, we assumed that four CLC proteins (PgCLC-B, PgCLC-C1, PgCLC-C2 and PgCLC-D) were CLC antiporters, while the other three PgCLCs (PgCLC-E, PgCLC-F and PgCLC-G) were likely CLC channels (Fig. 3A, B).

Gene strectures of *PgCLC* genes

The gene structure results showed that *PgCLC-C2*, *PgCLC-C1*, *PgCLC-G* and *PgCLC-B* contained five introns and six exons. *PgCLC-E* and *PgCLC-F* contained five exons and nine exons, respectively. A similar exon/intron structure profile, concerning intron number, intron phase, and exon length, was observed in *PgCLC-C2*, *PgCLC-C1* and *PgCLC-G*. In general, the *PgCLC* genes had a distinct intron-exon arrangement style (Fig. 4).

Growth characteristics and anion content in pomegranate tissues

With the increasing concentration of salinity, the dry weights of roots and stems showed no significant changes among each treatment (Table S4, $p < 0.05$). The leaf weight and total dry weight first increased and then decreased, reaching a peak at the 100 mM salinity level.

As shown in Figure 5A, the contents of Cl^- in pomegranate roots, stems and leaves significantly increased with the increasing concentration of salinity ($p < 0.05$). Under 300 mM NaCl stress, the levels of Cl^- in roots, stems and leaves increased 6.19, 5.29 and 7.42 times, compared with the control, respectively. The contents of Cl^- in plant tissues was ranked as leaf > stem > root. The NO_3^- contents in roots first increased

and then decreased, with the highest value at 100 mM salinity. However, the NO_3^- contents in stems and leaves had no obvious changes (except NO_3^- content in stem at 300 mM NaCl, $p < 0.05$) among the different treatments. The NO_3^- contents in plant tissues was ranked as root > stem > leaf (Fig. 5B). By contrast, the $H_2PO_4^-$ contents in roots increased along with the increaseing salinity, while no significant changes were observed in most leaf and stem samples ($p < 0.05$). Moreover, we found that $H_2PO_4^-$ was mainly accumulated in stems (Fig. 5C). First an increase and then a decrease of the SO_4^{2-} contents in roots and leaves were observed with peaks at 100 mM salinity. The leaf content of SO_4^{2-} fell sharply under higher salinity (> 200 mM NaCl). The results demonstrated that the accumulation of SO_4^{2-} mainly occurred in roots (Fig. 5D).

Expression patterns of *PgCLC* genes under NaCl stress

To further investigate the expression patterns of *PgCLCs*, we performed the qRT-PCR analysis in pomegranate roots and leaves. The results showed that all the *PgCLC* genes had tissue-specific expression patterns, with high expression levels in leaves and low expression levels in roots (Fig. 6). Notably, when plants were subjected to salinity, the expression levels of all the tested *PgCLCs* were upregulated in pomegranate leaves, but were down-regulated or not obviously changed in roots ($p< 0.01$). For instance, the relative expression levels of *PgCLC-B*, *PgCLC-C1*, *PgCLC-C1* and *PgCLC-D* in leaves increased with the increasing salinity; meanwhile, those of *PgCLC-E*, *PgCLC-F* and *PgCLC-G* in leaves significantly increased at high salinity (200 mM). Also, the expression levels of *PgCLC-B*, *PgCLC-F* and *PgCLC-G* in roots decreased and those of *PgCLC-C1*, *PgCLC-C2*, *PgCLC-D* and *PgCLC-E* in roots first decreased at 100 mM salinity level and then recovered slightly at 200 mM and/or 300 mM salinity levels (Fig. 6). Under 300mM NaCl stress, the expression levels of *PgCLC-C1*, *PgCLC-C2* and *PgCLC-F* in leaves increased by more than 16-fold relative to those of the controls.

Correlation between the anion contents and the expression levels of *PgCLC* genes

Correlation analysis showed that the *PgCLC* genes were positively correlated with each other (Fig. 7, $p < 0.05$). The Cl^- content had significantly positive correlations with *PgCLC-B*, *PgCLC-C1*, *PgCLC-C2* and *PgCLC-D*, while the SO_4^{2-} content had significantly negative correlations with these genes. Meanwhile, the contents of Cl^- and SO_4^{2-} were negatively correlated with each other ($p < 0.05$). A significantly negative correlation between the NO_3^- content and the expression level of *PgCLC-B*, and a significantly positive correlation between the SO_4^{2-} were found. There was no significant relationship between the $H_2PO_4^-$ content and the other indexes (Fig. 7). These findings suggested that accumulation of Cl^-, SO_4^{2-} and NO_3^- in pomegranate tissues was associated with the expression levels of *PgCLC* genes under salt stress.

Discussion

Identification of the CLC gene family in pomegranate

The CLC gene family is an evolutionarily well-conserved family, which has been found in prokaryotes and eukaryotes [9, 14]. CLC channels form two-pore homodimers with two monomers, and each monomer has its own pore through which Cl^- and other anions (HCO_3^-, I^-, and NO_3^-) may be conducted [9, 33]. CLC transporters and channels have regulatory functions when ATP, ADP, AMP, or adenosine are bound at the CBS domains [33]. In pomegranate, each CLCs contains one voltage-gated CLC domain near the N-terminus and two CBS domains at the C-terminus. The specific effect implies that individual CLC transporters and channels are sensitive to the cell's metabolic state [9, 22]. We found that PgCLCs were all hydrophobic proteins with numerous transmembrane helices (TMs) that were associated with their functions of allowing ion transport through membranes [34]. Also, PgCLC-E was found to be located on the chloroplast thylakoid membrane and might be related to photosynthesis activity, which was consistent with previous studies on AtCLCe by Marmagne *et al* [29].

Phylogenic relationships of the CLC gene family

Numerous early whole-genome duplication (WGD) events in plants, including the gamma event shared by core-eudicots [35], the WGD event shared by angiosperms [36-38], and the seed-plant WGD event [36, 37], contribute to gene duplications. The diversity of gene copy numbers from different lineages (Fig.1A) might be related to the rounds of WGD events shared with the taxon [39]. Based on the phylogenic analysis of the CLC gene family in 15 land plants, seven PgCLCs were divided into two clades, with clade I belonging to a eukaryotic branch and the clade II belonging to a bacterial branch [28, 29]. The divergence of clade I and clade II might have occurred before the origin of land plants due to each clade consisting of taxa from embrophytes (Fig. 1). The CLCs topology was consistent with that of *Arabidopsis* [28, 29], tobacco [40], tea (*Camellia sinensis*) [19] and trifoliate orange [18]. Phylogenetic analysis also indicated multiple rounds of ancient gene expansion (Fig. 1). For example, the gene duplication between CLC-C1 and CLC-C2 (the red star in Fig.1B) was supported by the duplication burst shared by core eudicots [41]. The gene duplication between the CLC-C and CLC-G subfamilies was due to one duplicate shared with angiosperms (the purple star in Fig.1B) [41]. Our phylogenetic analyses also found a gene expansion in seed plants, with a gene birth from an ancient gene duplication (the green star in Fig.1B) and a subsequent gene death. The CLC-A/B/C/G genes (Fig.1) exhibited a gene loss event in gymnosperms after experiencing the seed-plant WGD event [36, 37] despite the fact that the absence of the gene might have resulted from the putative incompleteness of the genome assembly and annotation. Recent phylogenetic studies have also found land plant-scale gene birth and expansion, such as in the CYP75 gene family [39] and GH28 gene family [36].

Additionally, the distributions of conserved motifs and conserved regions were consistent with the phylogenetic relationships (Fig. 2). Three highly conserved regions of the CLC gene family, GxGIPE (I), GKxGPxxH (II) and PxxGxLF (III) were shared by the members of clade I, whereas thesy were not shared by the members of clade II. This finding indicated that the divergence of clades I and clade II might be due to the presence of these conserved regions (Fig. 2C). Our study also found that the x residue in conserved region (I) of the CLC-A/B subfamily was P [proline, Pro] (Fig. 3; Fig. S2), which preferentially transports NO_3^- [20], while that of the CLC-C, CLC-D and CLC-G subfamily was S [serine, Ser] (Fig. 3; Fig. S2), which

preferentially transports Cl^- [20]. Thus, PgCLC-B is likely a NO_3^-/H^+ exchanger that mainly transports NO_3^- rather than Cl^- [16, 27], while PgCLC-C, PgCLC-D and PgCLC-G have high affinity for Cl^- [16, 27]. The presence of a gating glutamate (E) residue and proton glutamate (E) residue was a signature for CLC antiporters [21, 22]. However, if one or both of the Glu (E) residues were substituted by any other amino acids in the conserved region, the CLC proteins might exhibit CLC channels activity [22]. Therefore, we assumed that PgCLC-B, PgCLC-C1, PgCLC-C2 and PgCLC-D were CLC antiporters and the PgCLC-E, PgCLC-F and PgCLC-G were CLC channels. Our results were in line with the findings in *Arabidopsis* [21, 22].

PgCLCs played roles in the anion accumulation under NaCl stress

As an essential micronutrient for plants, chloride (Cl^-) is beneficial for plants at low concentrations in media [1, 2]. However, high salinity (mainly NaCl) may cause a perturbation of Na^+ and Cl^- at both the cellular and whole plant levels [42], which affects the uptake and transport of other mineral ions, such as K^+, Ca^{2+}, Mg^{2+}, $H_2PO_4^-$, NO_3^- and SO_4^{2-} [43, 44]. In this study, we focused on the anion accumulation in pomegranate tissues. CLC proteins are expressed on the cell membrane and conduct Cl^- or other anions, such as HCO_3^-, I^-, and NO_3^- [9-12]. Compared with the controls, the expression levels of the *PgCLCs* were upregulated in leaves and downregulated or not significantly changed in roots ($p < 0.01$). The tissue-specific expression of seven *PgCLCs* indicated different mechanisms of anions transport in pomegranate roots and leaves. Our study found that the Cl^- contents in pomegranate tissues sharply increased with an order of leaf > stem > root (Fig. 5A), indicating a relatively strong ability for the pomegranate to transport and accumulate toxic ions in the acrial parts [45]. In leaves, the high expression levels of *PgCLCs* suggested the inclusion of Cl^- into leaf cells. Individually, the expression levels of three antiporters *PgCLC-C1*, *PgCLC-C2* and *PgCLC-D* were significantly positive with the Cl^- content, which might be contributed to the sequestration of Cl^- into leaf vacuoles [23, 46]. However, the low expression levels of *PgCLCs* in roots suggested the exclusion of Cl^- from root cells. The recovery of *PgCLC-C1*, *PgCLC-C2* and *PgCLC-D* in roots were contributed to the sequestration of Cl^- into the root vacuoles at high salinity levels [23, 46]. Therefore, *PgCLCs* are believed to alleviate the deleterious effects of Cl^- via excluding the Cl^- from root cells and sequestrating Cl^- into leaf vacuoles [23, 46]. Similarly, some halophytes prefer to transport and accumulate detrimental ions in the acrial parts under salt stress [47, 48]. On the other hand, the low expression levels of *PgCLC-E*, *PgCLC-F* and *PgCLC-G* coding Cl^- channels in leaves at moderate salinity levels ($\leq$ 200 mM NaCl Fig. 7), suggested the capacity for pomegranate to inhibit the Cl^- influx into organelles, such as chloroplast and Golgi apparatus [8, 29].

Additionally, the NO_3^- contents of pomegranate roots first increased and then decreased, and that of leaves not changed under salt stress (Fig. 5B, D). The increases of the Cl^- contents were concomitant with the decreases of the NO_3^- contents in pomegranate tissues, which could be due to the antagonism between Cl^- and NO_3^- [49]. The expression level of *PgCLC-B* (a NO_3^-/H^+ exchanger) [16, 27], was significantly positive correlated with the Cl^- contents, and significantly negative correlated with the NO_3^- content ($p < 0.05$). These results suggested that the decreased uptake of NO_3^- in roots might be due to the inhibition of *PgCLC-*

B activity under salt stress [16, 27]. The inhibition of nitrogen uptake was also associated with nitrate transporter (NRTs) [50, 51]. Meanwhile, the increased expression level of *PgCLC-B* in leaves indicated an acceleration of transporting NO_3^- into leaves to mitigate the nitrogen deficiency [27]. Teakle *et al*. [3] reported that the increased concentration of NO_3^- in media reduced the Cl^- content in leaves and then mitigated the foliar salt damage, the NO_3^-/Cl^- even equaled to the K^+/Na^+, which was confirmed as one of the critical determinants of plant salt resistance [52, 53]. In pomegranate, it was observed that a low ratio of NO_3^-/Cl^- might cause a reduction in growth [54] (data not showed).

In a ward, these findings suggested that *PgCLC* genes played important roles in balance of Cl^- and NO_3^- in pomegranate tissues under salt stress [10-12, 23]. While the accumulation pattern of SO_4^{2-} was associated with the other genes, such as sulfate transporters [55]. Wei *et al*. [18] found that *PtrCLC* genes were dramatically induced in response to NaCl stress, and *PtrCLC6* showed a leaf-specific expression pattern in trifoliate orange. Zhang *et al*. [40] observed that all of the expressed *NtCLC* genes had a low expression level in tobacco roots under salt stress. Our findings are consistent with these reports. In addition, the functional characterization of each *PgCLC* genes need to further study.

Conclusions

In this study, we identified and characterized seven *CLC* genes in pomegranate. Phylogenetic analysis indicated that the PgCLCs were divided into two distinct clades, with a similar distribution of motifs and conserved regions in members of each clade. In pomegranate, the *PgCLC* genes displayed a tissue-specific expression pattern, with the high expression levels in leaves and the low expression levels in roots under salt stress. *PgCLC* genes are believed to play important roles in balance of Cl^- and NO_3^- in pomegranate tissues under salt stress. Our study provides the basis for the further functional characterization of the *PgCLC* genes.

Methods

Identification of the CLC gene family in pomegranate

A Hidden Markov Model (HMM) profile of the voltage-gated chloride channel (Voltage-gate CLC) domain (Accession no. PF00654) was employed to identify the putative CLC proteins from genome sequences using the software HMMER v3.1b1 [56] accorrding to the methods of Zhang *et al*. [39] with a cut-off E-value of $\leq 1e^{-10}$. To construct a representative phylogeny across land plants, ten angiosperms (eight core eudicots and two monocots), two gymnosperms and three bryophytes were selected, including *Arabidopsis thaliana*, *Citrus sinensis*, *Eucalyptus grandis*, *Eutrema salsugineum*, *Glycine max*, *Populus euphratica*, *Punica granatum*, and *Vitis vinifera* as the core eudicots; *Oryza sativa* and *Zostera marina* as monocots; *Ginkgo biloba* and *Pinus taeda* as gymnosperms; and *Marchantia polymorpha*, *Selaginella moellendorffii* and *Sphagnum fallax* as bryophytes. Seven CLC proteins from *Arabidopsis thaliana* were obtained from the Arabidopsis Information Resource (TAIR) (http://www.arabidopsis.org/). The genome sequences of 14 other species were downloaded from URLs (Table S1). Firstly, all the putative CLC proteins were identified

from the genomes of the 14 species. Subsequently, the CLC candidates were manually curated, and the nonredundant CLC proteins were further analyzed using the NCBI Conserved Domain Database (CDD, http://www.ncbi.nlm.nih.gov/cdd/) and SMART programs (http://smart.embl-heidelberg.de/) to confirm the presence of the Voltage-gate CLC domain. The theoretical isoelectric point (pI), molecular weight (Mw) and grand average of hydrophobicity (GRAVY) of seven PgCLC proteins were predicted using the Prot-Param tool (http://web.expasy.org/protparam/). The number of transmembrane helices (TMs) was predicted using TMHMM Server v. 2.0 (http://www.cbs.dtu.dk/services/TMHMM/) and TMpred (https://embnet.vital-it.ch/software/TMPRED_form.html). Subcellular localization was inferred with WoLF PSORT II (https://www.genscript.com/wolf-psort.html?src=leftbar).

Phylogenetic analysis of CLC gene family

To estimate the origin and divergence of CLC genes, an maximum likelihood (ML) tree of these genes was reconstructed using iQ-TREE and used to map on a species tree of land-plants, which is a part of the tree of life as inferred in the OneKP project [36], by using the methods in Zhang *et al* [57]. All of the puative CLC proteins were aligned using MUSCLE v3.8.31 [58] with the 'auto' setting. To improve the valid phylogeny signals, the low-quality alignment regions and incorrect sequences with apparent splice variants were removed [59]. Finally, a total of 113 putative CLC candidates were retained, including seven PgCLCs (Table S2). The conserved blocks were retained by Gblocks v0.91b [60], and then, phylogenetic analysis was preformed using iQ-TREE v2 [61] with the LG+R6 model, 1000 bootstraps, and the Shimodaira-Hasegawa-like aLRT (SH-aLRT) test. Putative functional homologs were identified from a gene clade that contained the query gene from *Arabidopsis* and was likely derived from an ancestral gene from land plants [57].

Conserved motifs, residues and gene stuctures prediction of CLC proteins

The conserved motifs and regions of all CLC proteins were predicted by the MEME tool (http://meme-suite.org/tools/meme). The maximum number of motifs was set to 10, and the optimum motif width was ≥ 6 and ≤ 50. Three conserved regions (GxGIPE (I), GKxGPxxH (II) and PxxGxLF (III)) of the CLC gene family were searched by the MAST tool (http://meme-suite.org/tools/mast) with a sequence threshold ≤ 30 and an E-value $\leq 1e^{-10}$ for motifs. Multiple sequence alignment of CLCs was performed by Clustal X v2.0 [62] and visualized by Jalview v1.0 [63]. The gene structure information of each *PgCLCs* was retrieved from the pomegranate genome and visualized using GSDS software (http://gsds.cbi.pku.edu.cn/).

Plant materials and growth conditions

Pomegranate cv. 'Taishanhong' cuttings (one-year-old, collected from Pomegranate repository of Nanjing Forestry University. China) were planted in a phytotron for six months, with a 28/22 °C day/night temperature, 60% humidity and 14 h light/10 h dark photoperiod. Hoagland's nutrient solution [64] was supplied at the beginning of the experiment. A total of 24 pots (one plant per plot) were arranged in a completely randomized 3 blocks, and 8 pots per block, and every 2 pots were designed as a biological replicate. All plants were fertigated with half-strength Hoagland's solution containing 0 (control), 100, 200, or 300 mM NaCl every six days, respectively. A saucer was placed under the containers to keep the soil moist. After 18 days of treatments, we harvested all plants separately to collect roots, stems, and leaves.

Anion content measurement

The dry weights of pomegranate roots, stems and leaves were determined after drying in a heating oven at 75 °C for 48 h. Dry samples were finely milled to pass through a 40-mesh sieve. Then 0.4 g of samples were treated with 50 mL of deionized water for 1 h in an ultrasonic extractor at room temperature, and then the obtained extracts were used to determine the contents of Cl^-, NO_3^-, $H_2PO_4^-$, and SO_4^{2-} using an ion chromatography (ICS900 ion chromatographic system; AS4A-SC ion-exchange column, CD M-II electrical conductivity detector, mobile phase: $Na_2CO_3/NaHCO_3$ = 1.7/1.8 mM; Dionex, Sunnyvale, USA) [65].

Expression levels of *PgCLCs* by quantitative real-time PCR (qRT-PCR)

Total RNA was extracted from fresh root and leaf samples using the BioTeke plant total RNA extraction kit (BioTeke Corporation, Beijing, China) according to the manufacturer's instructions. First-strand cDNA was prepared using a reverse transcription kit-PrimeScript^{TM} RT reagent Kit with gDNA Eraser (TaKaRa Bio Tech Co., Ltd., Beijing, China). The primers of seven *PgCLCs* were designed with NCBI primer-BLAST (Table S2). Real-time RT-PCR (qRT-PCR) was performed using a 7500 fast Real-Time PCR system (Applied Biosystems, CA, USA) with three biological and three technical replicates for each cDNA sample, and the results were quantitatively analyzed by the $2^{-\Delta\Delta CT}$ method [66]. Each reaction was carried out in a final volume of 20 μL, containing 10 μL of TB Green *Premix Ex Taq*, 0.4 μL of ROX Reference Dye II, 0.8 μL of upstream/downstream primers, 1 μL of cDNA template and 7 μL of ddH_2O. The PCR thermal cycler was set as follows: pre-denaturation at 95°C for 30 s; 40 cycles of 95°C for 5 s and 60°C for 34 s; the dissociation stage was set as follows: 95°C for 15 s, 60°C for 60 s and 95°C for 15 s. Pomegranate *PgActin* was used as an internal reference gene.

Data analysis

All data of the anion contents and qRT-PCR were analyzed with one-way ANOVA, and multiple comparisons were evaluated with the Turkey test ($p < 0.01$) using the SPSS program (Version 19.0. Chicago, IL, USA) based on the values of three complete randomized blocks. The correlation among variables was analyzed based on the ion content and expressional level of *PgCLCs* and visualized by a 'corrplot' package in R [67].

Abbreviations

CLC: Chloride channel; CBS:Cystathionine Beta Synthase; Glu:glutamate; pI:Theoretical Isoelectric Point, Mw:Molecular Weight; GRAVY:Grand Average of Hydrophobicity; TMs:Transmembrane Helices; ML:Maximum Likelihood; WGD:Whole-genome Duplication; OneKP preoject:One Thousand Plant Project; SH-aLRT:Shimodaira-Hasegawa-like aLRT; qRT-PCR:Quantitative real-time polymerase chain reaction.

Declarations

Ethics approval and consent to participate

Not applicable.

Consent for publication

Not applicable.

Availability of data and materials

The datasets supporting the conclusions of this article are included within the article (and its additional files).

Competing interests

The authors declare that they have no competing interests.

Funding

This work was supported by the Initiative Project for Talents of Nanjing Forestry University (GXL2014070, GXL2018032), the Doctorate Fellowship Foundation of Nanjing Forestry University, and the Priority Academic Program Development of Jiangsu High Education Institutions (PAPD), the National Natural Science Foundation of China (31901341), the Natural Science Foundation of Jiangsu Province (BK20180768). These funding bodies took part in the design of the study and collection, analysis, and interpretation of data, and the writing of the manuscript, as well as in the open access payment.

Authors' contributions

CL and TZ analyzed and interpreted the phylogenetic analysis. YZ and JD performed the expression level examination of the stressed plants. CL was a major contributor in determining the ion content, analyzing data and writing the manuscript, and XZ and ZY revised the manuscript. All authors read and approved the final manuscript.

Acknowledgements

Not applicable.

References

1. Marschner P. Marschner's Mineral Nutrition of Higher Plants. 3rd ed. Australia: Academic press; 2012.
2. White PJ, Broadley MR. Chloride in soils and its uptake and movement within the plant: A Review. Ann Bot. 2001;88(6):967–88.
3. Teakle NL, Tyerman SD. Mechanisms of Cl^- transport contributing to salt tolerance. Plant Cell Environ. 2010;33(4):566–89.

4. Karaivazoglou NA, Papakosta DK, Divanidis S. Effect of chloride in irrigation water and form of nitrogen fertilizer on Virginia (flue-cured) tobacco. Field Crops Res. 2005;92(1):61–74.
5. Tregeagle JM, Tisdall JM, Tester M, Walker RR, Barrettlennard EG, Setter TL. Cl^- uptake, transport and accumulation in grapevine rootstocks of differing capacity for Cl^- exclusion. Funct Plant Biol. 2010;37(7):665–73.
6. Wei P, Wang L, Liu A, Yu B, Lam HM. *GmCLC1* confers enhanced salt tolerance through regulating chloride accumulation in soybean. Front Plant Sci. 2016;7(113):1082.
7. Holl D, Hatib K, Bar-Ya'Akov I. Pomegranate: botany, horticulture, breeding. Hortic Rev. 2009;35(2):127–91.
8. Liu C, Yan M, Huang X, Yuan Z. Effects of NaCl stress on growth and ion homeostasis in pomegranate tissues. Eur J Hortic Sci. 2020;85(1):42–50.
9. Lu S, Wang J, Chitsaz F, Derbyshire MK, Geer RC, Gonzales NR, et al. CDD/SPARCLE: the conserved domain database in 2020. Nucleic Acids Res. 2020;48(D1):D265–8.
10. Miller AJ, Fan X, Orsel M, Smith SJ, Wells DM. Nitrate transport and signalling. J Exp Bot. 2007;58(9):2297.
11. Amtmann A, Armengaud P, Salt DE, Williams L. Effects of N, P, K and S on metabolism: new knowledge gained from multi-level analysis. Curr Opin Plant Biol. 2009;12(3):275–83.
12. Gojon A, Nacry P, Davidian JC. Root uptake regulation: a central process for NPS homeostasis in plants. Curr Opin Plant Biol. 2009;12(3):328.
13. Jentsch TJ, Steinmeyer K, Schwarz G. Primary structure of *Torpedo marmorata* chloride channel isolated by expression cloning in *Xenopus oocytes*. Nature. 1990;348(6301):510–4.
14. Jentsch TJ. CLC chloride channels and transporters: from genes to protein structure, pathology and physiology. Crit Rev Biochem Mol. 2008;43(1):3–36.
15. Lurin C, Geelen D, Barbierbrygoo H, Guern J, Maurel C. Cloning and functional expression of a plant voltage-dependent chloride channel. Plant Cell. 1996;8(4):701–11.
16. De Angeli A, Monachello D, Ephritikhine G, Frachisse J, Thomine S, Gambale F, et al. The nitrate/proton antiporter *AtCLCa* mediates nitrate accumulation in plant vacuoles. Nature. 2006;442(7105):939–42.
17. Nakamura A, Fukuda A, Sakai S, Tanaka Y. Molecular cloning, functional expression and subcellular localization of two putative vacuolar voltage-gated chloride channels in rice (*Oryza sativa* L.). Plant Cell Physiol. 2006;47(1):32–42.
18. Wei Q, Gu QQ, Wang N, Yang C, Peng S. Molecular cloning and characterization of the chloride channel gene family in trifoliate orange. Biol Plantarum. 2015;59(4):645–53.
19. Xing A, Ma Y, Wu Z, Nong S, Zhu J, Sun H, et al. Genome-wide identification and expression analysis of the CLC superfamily genes in tea plants (*Camellia sinensis*). Funct Integr Genomic. 2020;20:497–508.
20. Zifarelli G, Pusch M. CLC transport proteins in plants. FEBS Lett. 2010;584(10):2122–7.
21. Lisal J, Maduke M. Proton-coupled gating in chloride channels. Philos T Roy Soc B. 2009;364(1514):181–7.

22. Accardi A, Picollo A. CLC channels and transporters: proteins with borderline personalities. Biochim Biophys Acta. 2010;1798(8):1457–64.
23. Jossier M, Kroniewicz L, Dalmas F, Le TD, Ephritikhine G, Thomine S, et al. The Arabidopsis vacuolar anion transporter, *AtCLCc*, is involved in the regulation of stomatal movements and contributes to salt tolerance. Plant J. 2010;64(4):563–76.
24. Wei Q, Liu Y, Zhou G, Li Q, Yang C, Peng SA. Overexpression of *CsCLCc*, a chloride channel gene from *Poncirus trifoliata*, enhances salt tolerance in *Arabidopsis*. Plant Mol Biol Rep. 2013;31(6):1548–57.
25. Jentsch TJ, Michael P. CLC chloride channels and transporters: structure, function, physiology, and disease. Physiol Rev. 2018;98(3):1493–590.
26. Jossier M, Kroniewicz L, Dalmas F, Thiec DL, Ephritikhine G, Thomine S, et al. The Arabidopsis vacuolar anion transporter, *AtCLCc*, is involved in the regulation of stomatal movements and contributes to salt tolerance. Plant J. 2010;64(4):563–76.
27. Fechtbartenbach JVD, Bogner M, Dynowski M, Ludewig U. CLC-b-mediated NO_3^-/H^+ exchange across the tonoplast of *Arabidopsis* vacuoles. Plant Cell Physiol. 2010;51(6):960–8.
28. Barbierbrygoo HLN, Angeli AD, Filleur S, Frachisse JM, Gambale F, Thomine SB, et al. Anion channels/transporters in plants: from molecular bases to regulatory networks. Annu Rev Plant Biol. 2011;62(62):25–51.
29. Marmagne A, Vinaugerdouard M, Monachello D, De Longevialle AF, Charon C, Allot M, et al. Two members of the *Arabidopsis* CLC (chloride channel) family, *AtCLCe* and *AtCLCf*, are associated with thylakoid and Golgi membranes, respectively. J Exp Bot. 2007;58(12):3385–93.
30. Guo W, Zuo Z, Cheng X, Sun J, Li H, Li L, et al. The chloride channel family gene *CLCd* negatively regulates pathogen-associated molecular pattern (PAMP)-triggered immunity in *Arabidopsis*. J Exp Bot. 2014;65(4):1205–15.
31. Tam NC, Astrid A, Mathieu J, Sylvain D, Sébastien T, Sophie F. Characterization of the chloride channel-like, *AtCLCg*, involved in chloride tolerance in *Arabidopsis thaliana*. Plant Cell Physiol. 2016;57(4):764–75.
32. Wei P, Che B, Shen L, Cui Y, Wu S, Cheng C, et al. Identification and functional characterization of the chloride channel gene, *GsCLC-c2* from wild soybean. BMC Plant Biol. 2019;19(1):1–15.
33. Elgebali S, Mistry J, Bateman A, Eddy SR, Luciani A, Potter SC, et al. The Pfam protein families database in 2019. Nucleic Acids Res. 2019;47(D1):D427–32.
34. Kyte J, Doolittle RF. A simple method for displaying the hydropathic character of a protein. J Mol Biol. 1982;157(1):105–32.
35. Jaillon O, Aury J, Noel B, Policriti A, Clepet C, Casagrande A, et al. The grapevine genome sequence suggests ancestral hexaploidization in major angiosperm phyla. Nature. 2007;449(7161):463–7.
36. Initiative OTPT. One thousand plant transcriptomes and the phylogenomics of green plants. Nature. 2019;574(7780):679–85.
37. Jiao Y, Wickett NJ, Ayyampalayam S, Chanderbali AS, Landherr L, Ralph PE, et al. Ancestral polyploidy in seed plants and angiosperms. Nature. 2011;473(7345):97–100.

38. Genome A. The Amborella Genome and the Evolution of Flowering Plants. Science. 2013;342(6165):1241089–9.
39. Zhang T, Liu C, Huang X, Zhang H, Yuan Z. Land-plant phylogenomic and pomegranate transcriptomic analyses reveal an evolutionary scenario of *CYP75* genes subsequent to whole genome duplications. Journal of plant biology. 2019;62(1):48–60.
40. Hui Z, Jin J, Jin L, Li Z, Xu G, Ran W, et al. Identification and analysis of the chloride channel gene family members in tobacco (*Nicotiana tabacum*). Gene. 2018;676:56–64.
41. Ren R, Wang H, Guo C, Zhang N, Zeng L, Chen Y, et al. Wide-spread whole genome duplications contribute to genome complexity and species diversity in angiosperms. Mol Plant. 2018;11(3):414–28.
42. Teakle NL, Tyerman SD. Mechanisms of Cl^- transport contributing to salt tolerance. Plant Cell Environ. 2010;33(4):566–89.
43. Silva EN, Silveira JA, Rodrigues CR, Viégas RA. Physiological adjustment to salt stress in Jatropha curcas is associated with accumulation of salt ions, transport and selectivity of K^+, osmotic adjustment and K^+/Na^+ homeostasis. Plant Biol. 2015;17(5):1023–9.
44. Ibrahim H. Tolerance of two pomegranates cultivars (*Punica granatum* L.) to salinity stress under hydroponic culture conditions. J Basic Appl Sci Res. 2016;6(4):38–46.
45. Munns R. Comparative physiology of salt and water stress. Plant Cell Environ. 2002;25(2):239–50.
46. Zhang H, Zhao F, Tang R, Yu Y, Song J, Wang Y, et al. Two tonoplast MATE proteins function as turgor-regulating chloride channels in *Arabidopsis*. P Natl Acad Sci USA. 2017;114(10):E2036–45.
47. Flowers TJ, Colmer TD. Salinity tolerance in halophytes. New Phytol. 2008;179(4):945–63.
48. Orsini F, Accorsi M, Gianquinto G, Dinelli G, Antognoni F, Carrasco KBR, et al. Beyond the ionic and osmotic response to salinity in *Chenopodium quinoa*: functional elements of successful halophytism. Funct Plant Biol. 2011;38(10):818–31.
49. Abdelgadir EM, Oka M, Fujiyama H. Nitrogen nutrition of rice plants under salinity. Biol Plantarum. 2005;49(1):99–104.
50. Wang H, Zhang M, Guo R, Shi D, Liu B, Lin X, et al. Effects of salt stress on ion balance and nitrogen metabolism of old and young leaves in rice (*Oryza sativa* L.). BMC Plant Biol. 2012;12(1):194–4.
51. Kiba T, Feria-Bourrellier A-B, Lafouge F, Lezhneva L, Boutet-Mercey S, Orsel M, et al. The *Arabidopsis* nitrate transporter NRT2.4 plays a double role in roots and shoots of nitrogen-starved plants. Plant Cell. 2012;24(1):245–58.
52. Apse MP, Blumwald E. Na^+ transport in plants. FEBS Lett. 2007;581(12):2247–54.
53. Munns R, Tester M. Mechanisms of salinity tolerance. Annu Rev Plant Biol. 2008;59(1):651–81.
54. Grattan S, Grieve C. Salinity–mineral nutrient relations in horticultural crops. Sci Hortic-Amsterdam. 1998;78(1–4):127–57.
55. Rouached H, Wirtz M, Alary R, Hell R, Arpat AB, Davidian JC, et al. Differential regulation of the expression of two high-affinity sulfate transporters, SULTR1.1 and SULTR1.2, in *Arabidopsis*. Plant Physiol. 2008;147:897–911.

56. Finn RD, Clements J, Eddy SR. HMMER web server: interactive sequence similarity searching. Nucleic Acids Res. 2011;39:29–37.
57. Zhang C, Zhang T, Luebert F, Xiang Y, Huang C-H, Hu Y, et al. Asterid phylogenomics/phylotranscriptomics uncover morphological evolutionary histories and support phylogenetic placement for numerous whole genome duplications. Mol Biol Evol. 2020.
58. Edgar RC. MUSCLE: multiple sequence alignment with high accuracy and high throughput. Nucleic Acids Res. 2004;32(5):1792–7.
59. Hartmann A, Tesch D, Nothwang HG, Binindaemonds ORP. Evolution of the cation chloride cotransporter family: ancient origins, gene-losses, and subfunctionalization through duplication. Mol Biol Evol. 2014;31(2):434–47.
60. Castresana J. Selection of conserved blocks from multiple alignments for their use in phylogenetic analysis. Mol Biol Evol. 2000;17(4):540–52.
61. Minh BQ, Schmidt HA, Chernomor O, Schrempf D, Woodhams MD, Von Haeseler A, et al. IQ-TREE 2: New models and efficient methods for phylogenetic inference in the genomic era. Mol Biol Evol. 2020;37(5):1530–4.
62. Larkin MA, Blackshields G, Brown NP, Chenna RM, Higgins DG. Clustal W and Clustal X Version 2.0. Bioinformatics. 2007;23(21):2947–8.
63. Clamp M, Cuff J, Searle SM, Barton GJ. The Jalview Java alignment editor. Bioinformatics. 2004;20(3):426–7.
64. Feng ZT, Deng YQ, Fan H, Sun QJ, Sui N, Wang BS. Effects of NaCl stress on the growth and photosynthetic characteristics of *Ulmus pumila* L. seedlings in sand culture. Photosynthetica. 2014;52(2):313–20.
65. Rui G, Shi LX, Yang YF. Germination, growth, osmotic adjustment and ionic balance of wheat in response to saline and alkaline stresses. Soil Sci Plant Nutr. 2009;55(5):667–79.
66. Livak KJ, Schmittgen TD. Analysis of relative gene expression data using real-time quantitative PCR and the $2^{-\Delta\Delta CT}$ Method. Methods. 2001;25(4):402–8.
67. Wei T, Simko V, Levy M, Xie Y, Jin Y, Zemla J. Package 'corrplot'. Statistician. 2017;56:316–24.

Figures

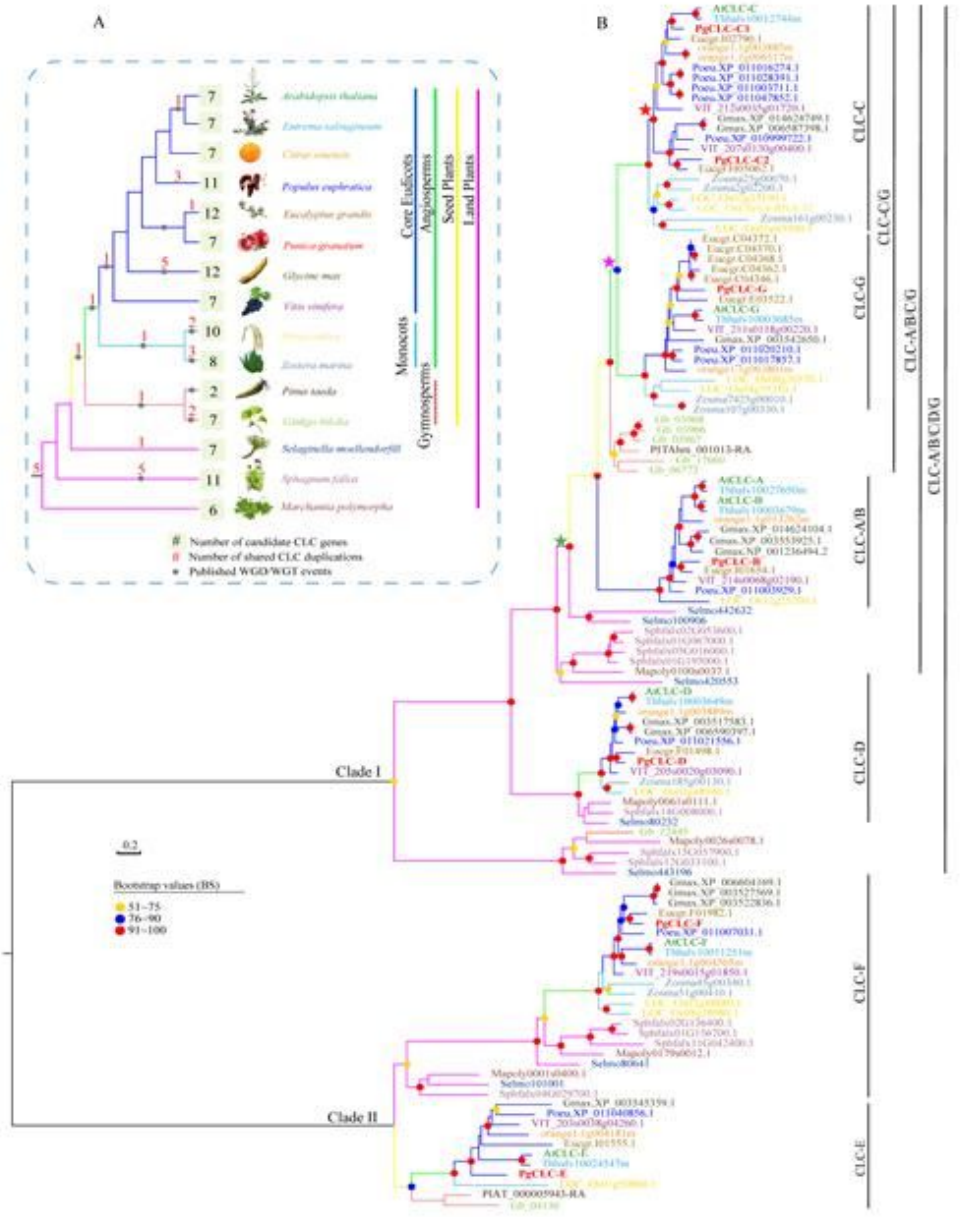

Figure 1

Phylogenetic analysis of the CLC gene family in land plants. (A) Species tree with different branch colors showing distinct species. (B) Phylogenetic tree of the CLC gene family in land plants presented in various branch colors, as in Figure A. Node support (pots) was quantified by aLRT statistics with the SH-like procedure. Colored stars are gene duplication events.

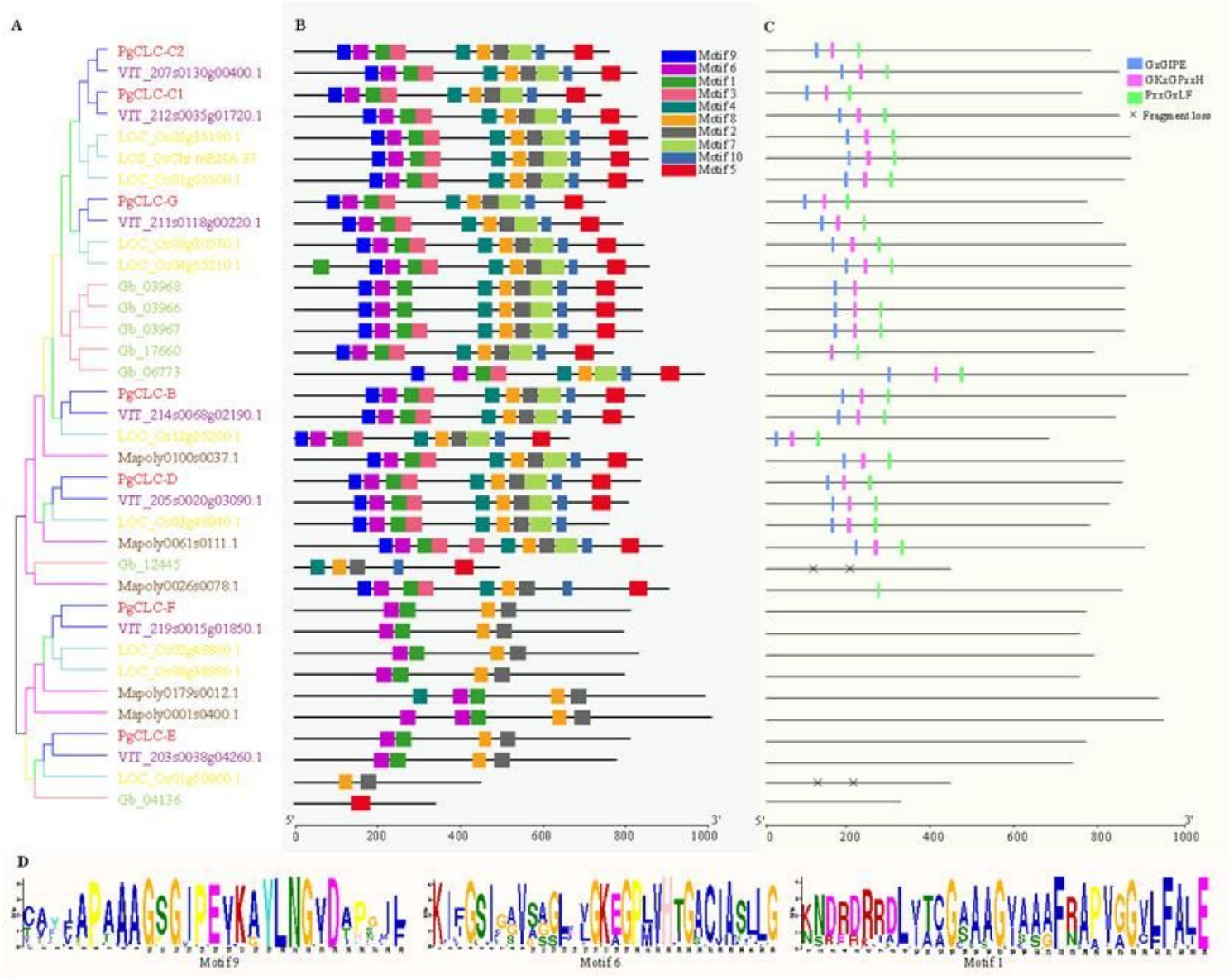

Figure 2

Phylogenetic tree of five species: Punica granatum, Vitis vinifera, Oryza sativa, Ginkgo biloba and Marchantia polymorpha (A), motif distribution of CLC proteins (B), three conserved regions in CLCs (C) and three typical motif logos (D). Three colored regions are present with their counterpart light-colored motifs, respectively.

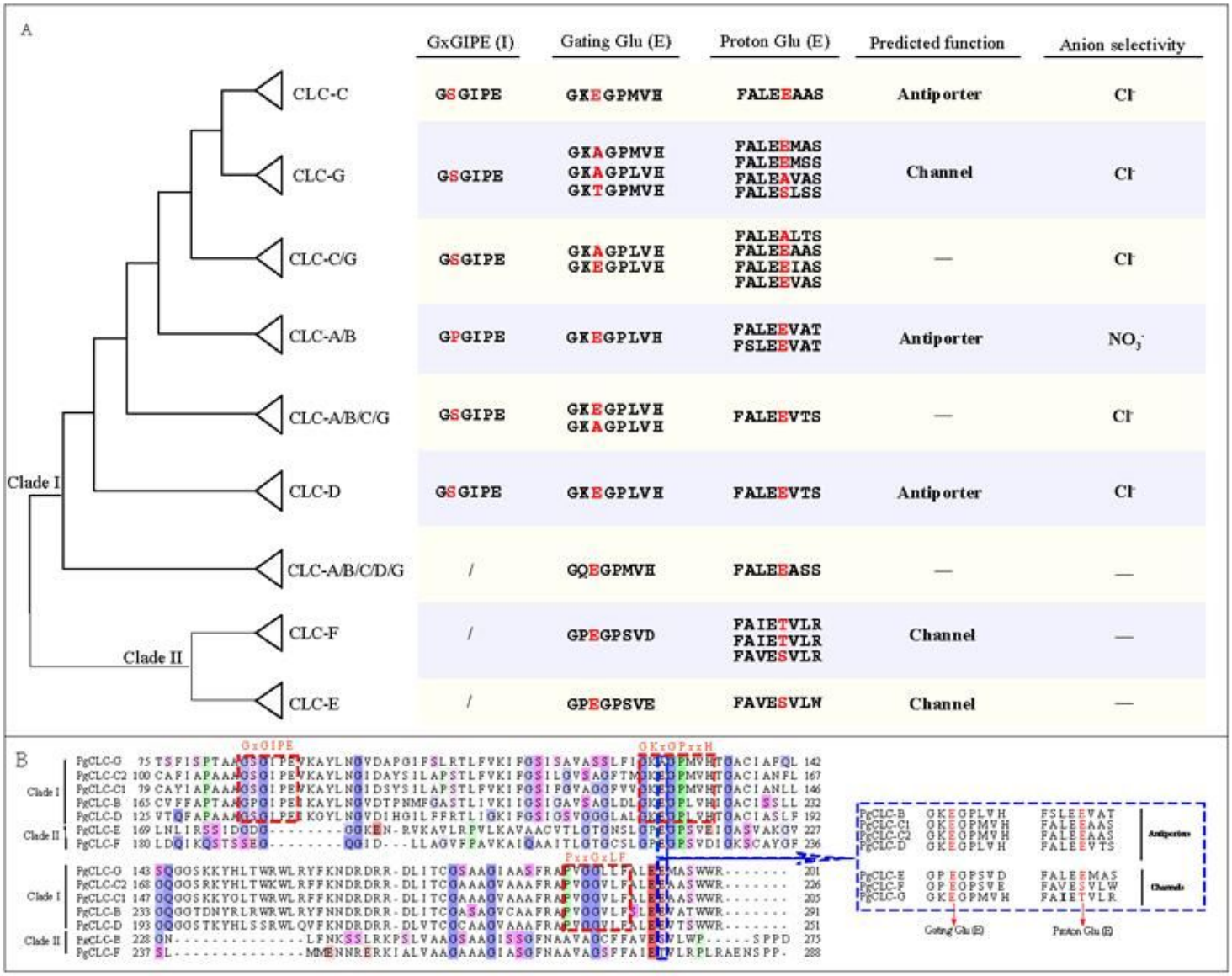

Figure 3

Conserved residues distribution in the CLC gene family. (A) CLC gene tree with collapsed branches, and the conserved residues of each subfamily are listed on the right. Distinct residues are highlighted in red. (B) Partial sequence alignment of the seven CLC proteins in pomegranate. The conserved regions: GxGIPE (I), GKxGPxxH (II) and PxxGxLF (III) are circled in red color. Conserved E (Glu) residues are circled in blue color. The presence of the conserved gating glutamate (E) and/or proton glutamate (E) residues is a signature for distinguishing the CLC antiporters and CLC channels, respectively.

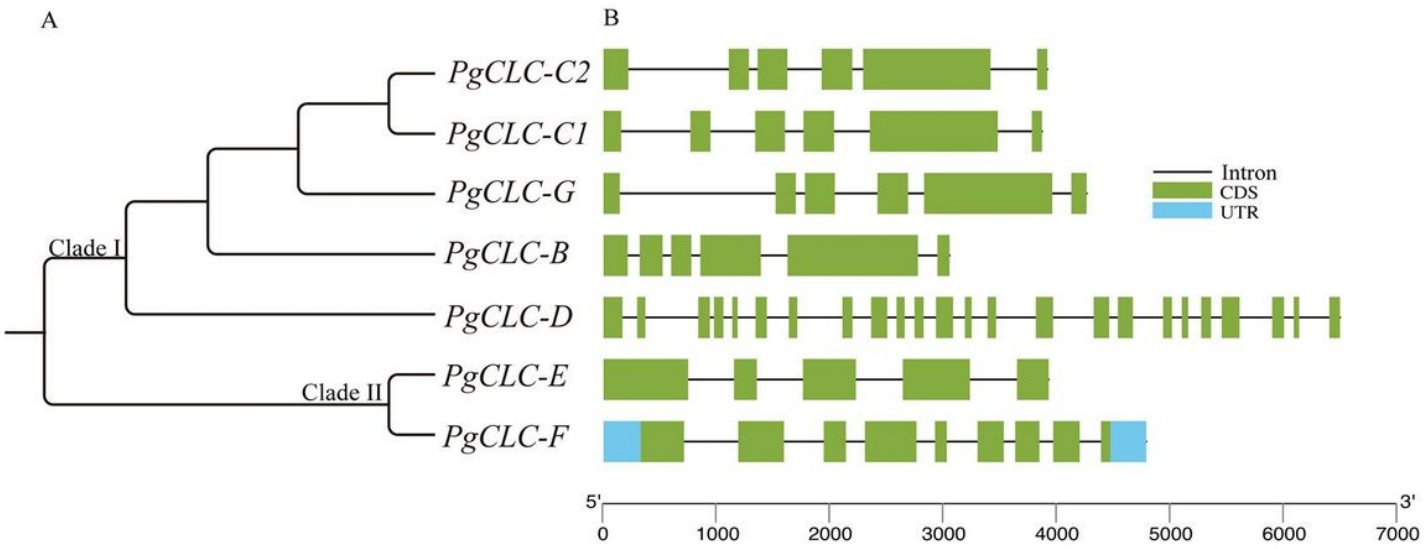

Figure 4

A PgCLCs tree derived from the CLC phylogenetic tree of 15 land plants (A), and the gene structures of PgCLCs (B).

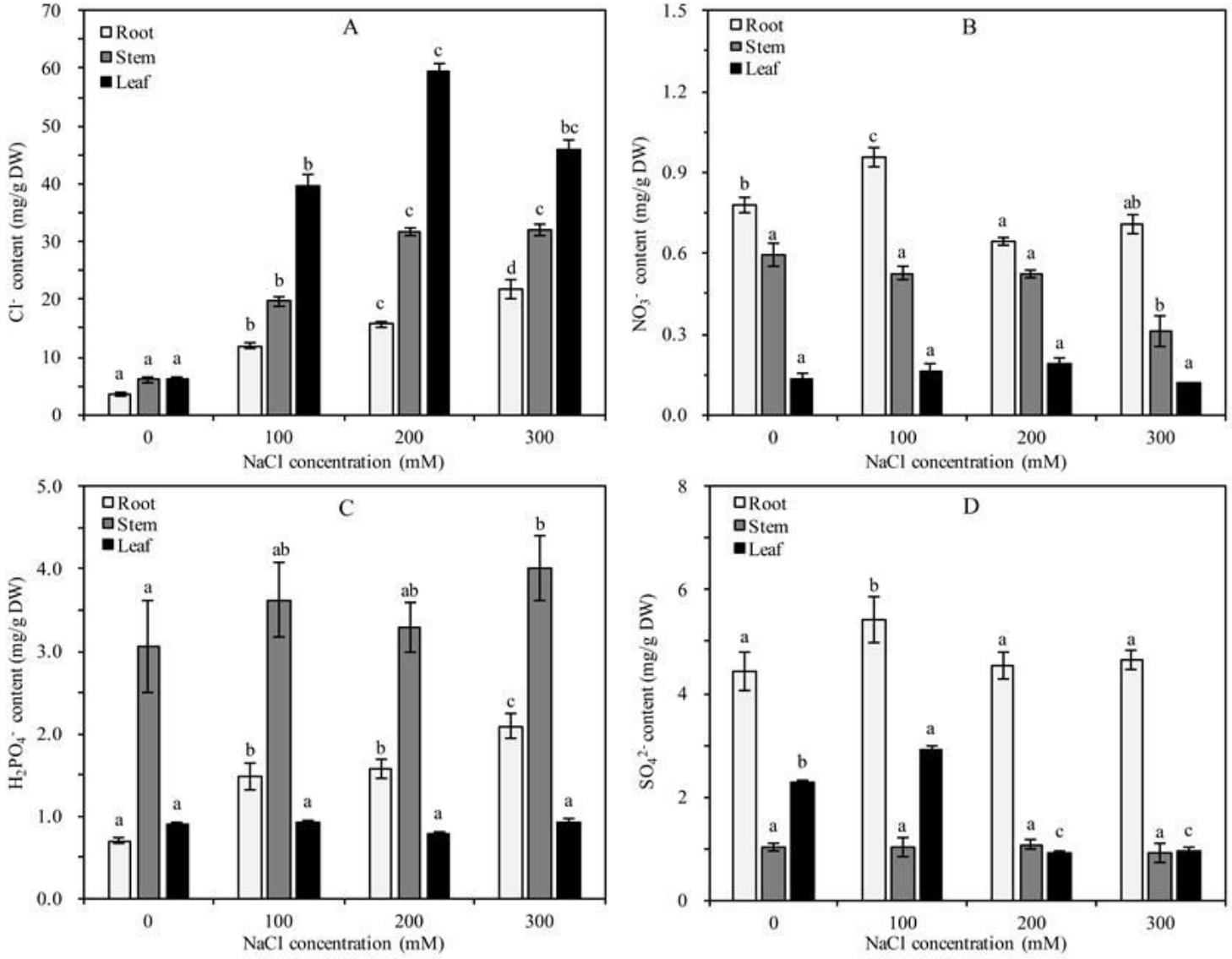

Figure 5

The concentrations of Cl− (A), NO3− (B), H2PO4− (C), and SO42− (D) in pomegranate tissues under NaCl stress. The values are the means ± SE of three replicates. Bars with different letters within each panel represent significant differences at $p < 0.05$.

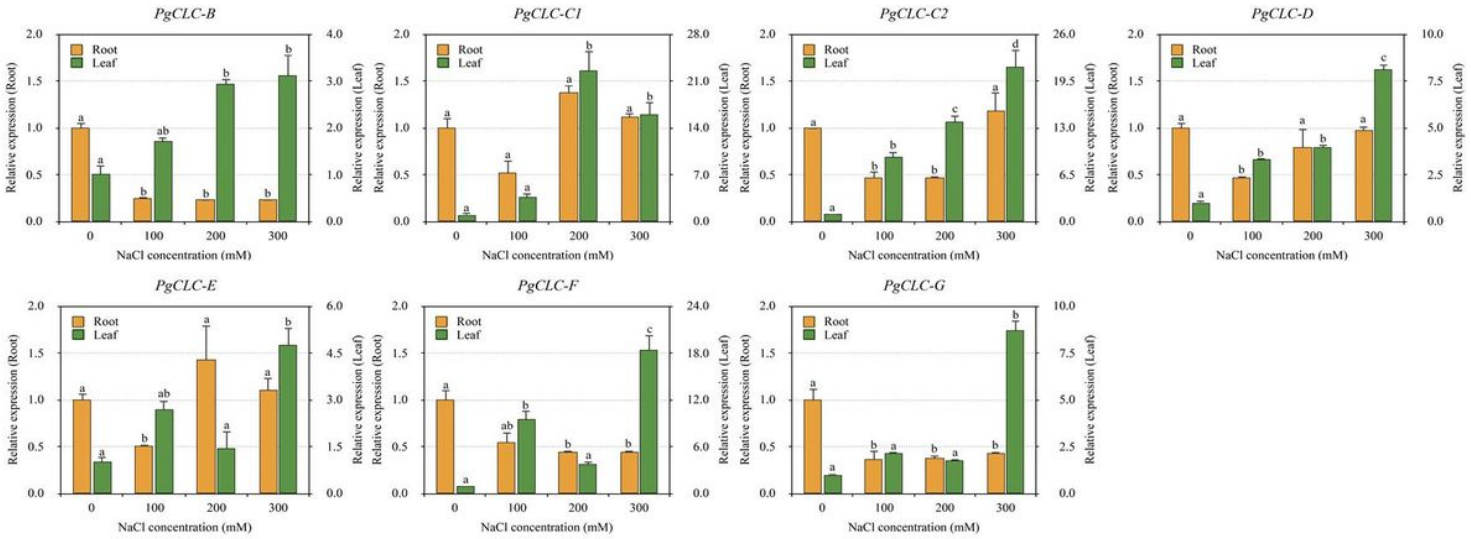

Figure 6

qRT-PCR analysis of the CLC genes in pomegranate roots and leaves after 18 days of NaCl stress, the expressional levels are calculated by the 2−ΔΔCT method. Bars with different letters within each panel are significantly different at $p < 0.01$.

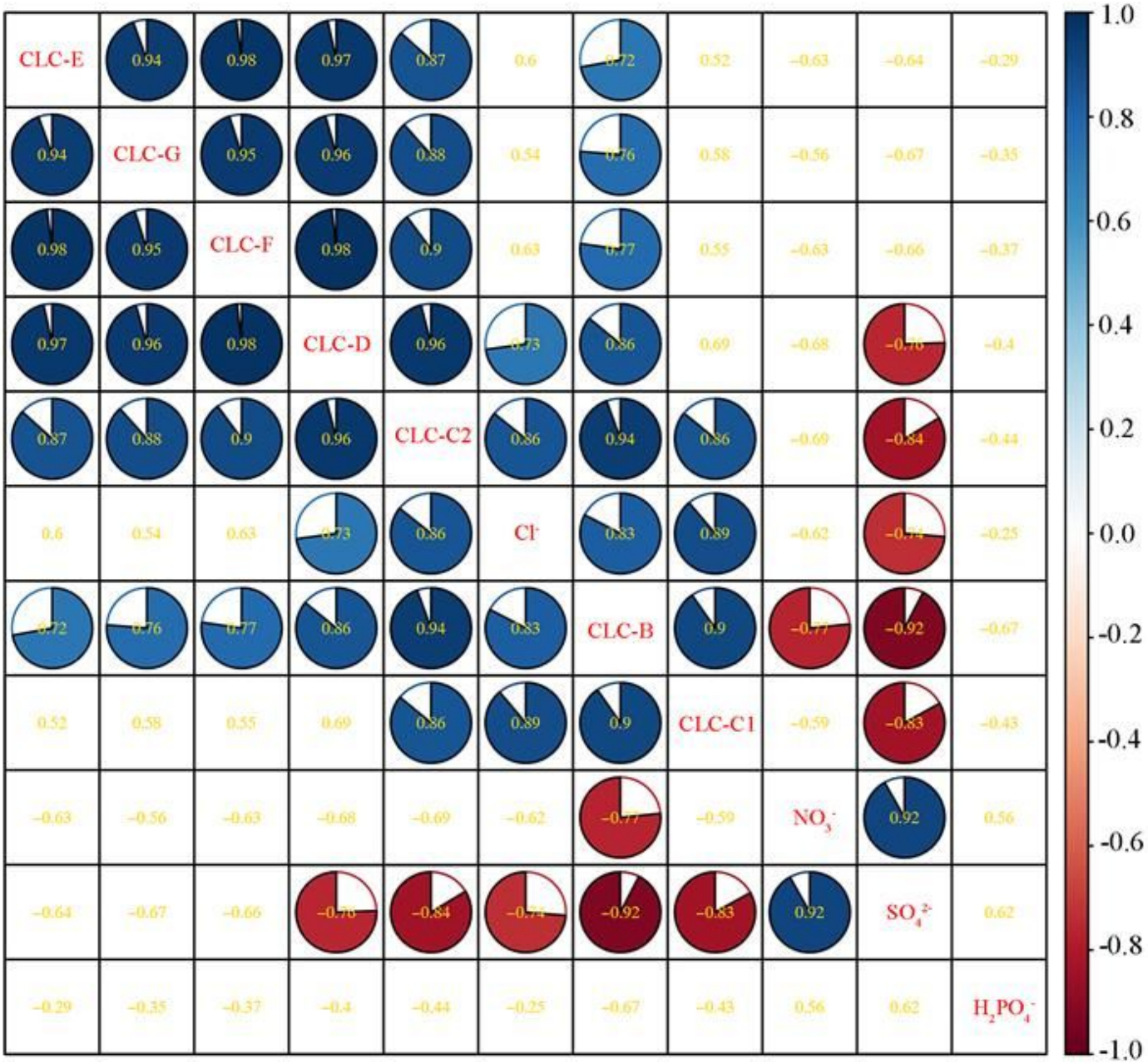

Figure 7

Correlations between the expression levels of seven PgCLCs and the anion contents of pomegranate roots and leaves. The blue pie indicates a positive correlation, and the red pie indicates a negative correlation. The darker the color, the more significant the correlation. Gold numbers ≥ 0.84 are highly significant at $p < 0.01$, and numbers ≥ 0.72 and < 0.84 are significant at $p < 0.05$.

Supplementary Files

This is a list of supplementary files associated with this preprint. Click to download.

- Additionalfile2.pdf

- Additionalfile1.xls